astro-ph/9509074 - UCLA-ASTRO-ELW-95-03

On the Density of PBH's in the Galactic Halo

Edward L. Wright
UCLA Dept. of Physics & Astronomy

ABSTRACT

Calculations of the rate of local Primordial Black Hole explosions often assume that the PBH's can be highly concentrated into galaxies, thereby weakening the Page-Hawking limit on the cosmological density of PBH's. But if the PBH's are concentrated by a factor exceeding $c/(H_\circ R_\circ) \approx 4 \times 10^5$, where $R_\circ = 8.5$ kpc is the scale of the Milky Way, then the steady emission from the PBH's in the halo will produce an anisotropic high latitude diffuse gamma ray intensity larger than the observed anisotropy. This provides a limit on the rate-density of evaporating PBH's of $\lesssim 0.4$ pc^{-3}yr^{-1} which is more than 6 orders of magnitude lower than recent experimental limits. However, the weak observed anisotropic high latitude diffuse gamma ray intensity is consistent with the idea that the dark matter that closes the Universe is Planck mass remnants of evaporated black holes.

Subject headings: gamma rays: observations – cosmology: dark matter – Galaxy: halo

1. Introduction

The average density of primordial black hole's (PBH's) in the Universe is constrained by the Page-Hawking (1976) limit on the diffuse gamma ray intensity, since the Hawking (1974) radiation from PBH's produces copious gamma rays. Halzen *et al.* (1991) computed the photon spectrum from a uniform density of PBH's with the initial mass function $n_i(m_i)dm_i \propto m_i^{-2.5}dm_i$, and found that $\Omega_{PBH}h^2 < (7.6 \pm 2.6) \times 10^{-9}$ with $h = H_\circ/100$ km/sec/Mpc, or an average mass density of PBH's of $\rho_{PBH} < 1.43 \times 10^{-37}$ gm cm^{-3}, and an average number density of PBH's of $N = 10^4$ pc^{-3}.

Now I wish to calculate the maximum allowed density of PBH's in the halo of the Milky Way. The halo mass density is given by

$$\rho_h = \frac{v_c^2}{4\pi G R^2} = 8.4 \times 10^{-25} \text{ gm cm}^{-3} \tag{1}$$

at the position of the solar circle, $R_\circ = 8.5$ kpc, for a circular velocity of $v_c = 220$ km/sec. Since the halo density is $(4.5 \times 10^4)/\Omega h^2$ times higher than the average density of the Universe, one

could hope that the PBH's would have a higher density in the halo of the Milky Way which would make it easier to detect the explosions caused by their final evaporation in high energy gamma ray experiments. In fact, Halzen *et al.* (1991) considered concentration factors up to $\zeta = \rho_h/\overline{\rho} = 1.36/h^2 \times 10^7$ by assuming that the PBH's were as highly concentrated as the luminous matter. Cline & Hong (1992) considered local densities as high as $N = 10^{12}$ pc^{-3} by assuming that some of the gamma-ray bursts observed by BATSE were PBH explosions.

2. Calculation of Anisotropy

However, the PBH's in the halo will contribute an anisotropic diffuse gamma ray intensity that will be much easier to measure for instrumental reasons than the isotropic intensity. A rough order of magnitude estimate for this anisotropic signal is a fraction $\zeta H_\circ R_\circ/c$ times the isotropic background. In order to improve this calculation, I need to compute the local average emissivity from the Page-Hawking limit which is integrated over time. For simplicity, I will do this calculation for the bolometric gamma ray intensity, though a frequency-dependent calculation would give a better limit. The mass spectrum of PBH's produced by a scale invariant perturbation spectrum in the early Universe is $n_i(m_i)dm_i \propto m_i^{-2.5}dm_i$, and the initial mass of a PBH that is evaporating at time t is $m_i \propto t^{1/3}$. The total comoving density $\rho/(1+z)^3$ of PBH's scales like

$$\rho/(1+z)^3 \quad \propto \quad \int_{t^{1/3}} m\, m^{-2.5} dm \quad \propto \quad t^{-1/6} \tag{2}$$

and thus the comoving luminosity density scales like $t^{-7/6} \propto (1+z)^{7/4}$ for $\Omega = 1$. The bolometric intensity is related to the comoving emissivity by

$$I = \int \frac{j_{CM}(t)}{1+z} c dt = \int \frac{j_\circ (1+z)^{7/4}}{(1+z)^{7/2}} \frac{c}{H_\circ} dz \tag{3}$$

This gives the relationship between the current average emissivity and the isotropic integrated intensity,

$$I_{iso} = \frac{4 j_\circ c}{3 H_\circ}. \tag{4}$$

Now I will calculate the emission from the halo of the Milky Way. If the emissivity of the halo is j_h, then its contribution to the anisotropic intensity at angle θ with respect to the Galactic center is

$$I_{aniso} = \int j_h(R) ds = \frac{\pi - \theta}{\sin\theta} j_h(R_\circ) R_\circ \tag{5}$$

for a spherical halo with density following the singular isothermal sphere model: $\rho \propto r^{-2}$. This is a special case of an "isothermal" halo with core radius r_c, flattening q, and density varying like:

$$\rho = \frac{\rho_\circ (R_\circ^2 + r_c^2)}{R^2 + z^2/q^2 + r_c^2} \tag{6}$$

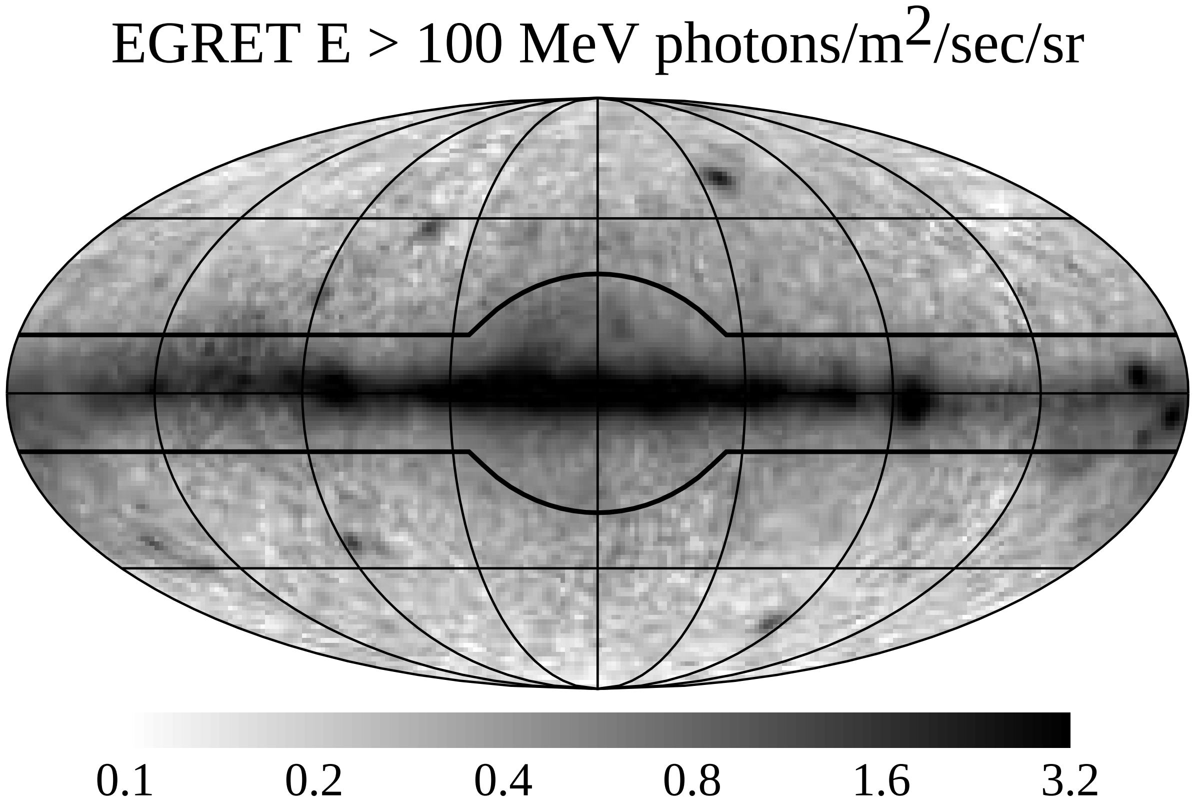

Fig. 1.— Gamma rays with $E > 100$ MeV from EGRET.

with R and z being cylindrical coordinates. This gives an anisotropic intensity of

$$I_{aniso} = \int j_h ds = j_h(R_\circ) R_\circ \eta(l, b, r_c/R_\circ, q) \tag{7}$$

with

$$\eta(l, b, r_c/R_\circ, q) = \frac{(1 + (r_c/R_\circ)^2)\left[\pi/2 + \tan^{-1}(\cos\theta'/\sin\theta'')\right]}{\sin\theta''\sqrt{1 + (q^{-2} - 1)\sin^2 b}} \tag{8}$$

where $\cos\theta' = (\cos l \cos b)/\sqrt{1 + (q^{-2} - 1)\sin^2 b}$ and $\sin\theta'' = \sqrt{1 - \cos^2\theta' + r_c^2/R_\circ^2}$.

Most of the uncertainty in the endpoint of primordial black hole evaporation cancels out in the ratio of I_{aniso}/I_{iso} which is given by

$$\frac{I_{aniso}}{I_{iso}} = \eta(l, b, r_c/R_\circ, q) \frac{j_h(R_\circ)}{j_\circ} \frac{3H_\circ R_\circ}{4c} \tag{9}$$

3. Comparison with Data

Using the combined Phase I EGRET sky maps in the directory /compton_data/egret/combined_data on legacy.gsfc.nasa.gov, I have constructed the rate

map in Figure 1. This shows the rate of gamma rays with $E > 100$ MeV. Figure 1 has been smoothed with a 2° FWHM quasi-Gaussian test function (Wright *et al.* 1994), but the fits are based on unsmoothed maps.

PBH's are not the only, or even the primary, source of galactic gamma ray emission. The process

$$p_{CR} + p_{ISM} \rightarrow p + p + \pi^\circ \rightarrow p + p + 2\gamma \tag{10}$$

where a cosmic ray proton p_{CR} hits an interstellar medium proton p_{ISM} is the dominant source of galactic gamma rays. Digel, Hunter & Mukherjee (1995) find an average emissivity of $(1.7 \pm 0.1) \times 10^{-26}$ photons/sec/sr/proton for $E_\gamma > 100$ MeV in the Orion region which is similar to interstellar medium emission rates elsewhere in the solar neighborhood. While the cosmic ray density appears to be higher in the inner galaxy, leading to a higher emissivity per ISM proton, I can avoid this complication by not using regions close to the galactic plane in my fits. I have used the 100 μm intensity as a proxy for the column density of ISM protons. This will automatically include the H_2 and H II components of the ISM that are not measured by the 21 cm neutral hydrogen line. The 100 μm emissivity per proton will depend on the local dust properties and radiation field, but avoidance of the galactic plane minimizes these complications as well. The 100 μm intensity at high $|b|$ is approximately 0.6×10^{-20} MJy/sr/proton/cm^2, so one expects about 0.03 photons/m^2/sr with $E > 100$ MeV for each MJy/sr of 100 μm intensity.

When I fit the gamma ray map to the form

$$I_\gamma(l,b) = j_h(R_\circ)R_\circ\, \eta(l,b,r_c/R_\circ,q) + \frac{dI_\gamma}{dI_{100}} I_{100}(l,b) + \frac{dI_\gamma}{d\csc|b|}\csc|b| + I_\circ + \epsilon(l,b) \tag{11}$$

with I_{100} being the 100 μm intensity from the DIRBE instrument on *COBE* with a model of the zodiacal light removed, and ϵ being the residual, I get the results shown in Table 1. Missing parameter values are fixed at their default values, which are zero except for $r_c/R_\circ = 0.01$ and $q = 1$ (which approximate the simple singular isothermal sphere model.) The isotropic intensity is required to be non-negative. These fits were done using the least sum of absolute errors $\sum|\epsilon|$ instead of least squares fitting to avoid the effect of bright sources, and an elliptical region surrounding the Galactic Center with $b = \pm 30^\circ$ and $l = \pm 45^\circ$ was excluded along with $|b| < 14.5^\circ$. The excluded region is marked on Figure 1. The pixels used for this fit were *COBE* DMR pixels with 4328 pixels outside the exclusion region, so differences in $\sum|\epsilon|$ greater than 0.1% are statistically significant. Simulating fits to 100 skies based on the best fit model in Table 1 along with the observed residuals gave values of $j_h(R_\circ)R_\circ$ with a standard deviation of 0.00165, which is negligible when compared to the range of $j_h(R_\circ)R_\circ$ obtained using different galactic tracers and halo models.

The coefficient found for the I_{100} term is consistent with the result expected from studies of the interstellar medium in the solar neighborhood (Digel *et al.* 1995), but when $\csc|b|$ or flattened haloes are allowed to absorb some of the galactic flux the coefficient is slightly lower but not unreasonable. Fits that do not include $\csc|b|$ as a tracer tend to favor flattened haloes with

large core radii, which makes the halo model η approximately proportional to $\csc|b|$. Models that do include a separate $\csc|b|$ term favor spherical, singular isothermal sphere haloes. Because a flattened halo has a smaller thickness at high $|b|$, the fitted halo density is higher for the flattened models. The large core radius in the flattened models causes the halo to produce a large monopole contribution to the intensity, so the isotropic term goes to zero in the flattened models.

Models similar to the large core radius spherical haloes proposed for gamma ray burst (GRB) sources do not provide an anisotropic intensity, for the simple reason that the GRB's are observed to be isotropic. In these models the halo density is limited by the isotropic intensity, and scales like $\jmath_h \propto r_c^{-1}$. Thus large core radius models are not significant for placing an upper limit on the local halo density.

Different methods of fitting for the galaxy give very different estimates for the isotropic background, but the estimate for the local halo density $j_h(R_\circ)$ is slightly more stable. Thus it is more appropriate to normalize to the Halzen *et al.*)1991) model upon which their calculation of the Page-Hawking limit is based instead of the uncertain isotropic background. Integrating Figure 3 of Halzen *et al.* (1991) for $E > 100$ MeV gives a flux of 0.06 photons/m^2/sec/sr which is in the range of the isotropic intensities from the fits in Table 1, and is also consistent with the darkest sky intensity of 0.15 photons/m^2/sec/sr given by Bertsch *et al.* (1995).

Comparing these results with Equation 9 implies that

$$\frac{j_h(R_\circ)R_\circ}{(4/3)j_\circ(c/H_\circ)} = \frac{0.023\text{–}0.15}{0.06} = 0.4\text{–}2.5 \tag{12}$$

or

$$\zeta = \frac{4c}{3H_\circ R_\circ} \times 0.4\text{–}2.5 = (2\text{–}12)/h \times 10^5. \tag{13}$$

Using this ζ I get a local density of PBH's of $N_h = \zeta \times 10^4 = (2\text{–}12)/h \times 10^9$ pc^{-3}.

An alternative fit is shown in Figure 2. The data with $|b| > 19.3^\circ$ was binned into twenty bins equally spaced in $\cos\theta$. Within each bin, the mid-average, or average of the two middle quartiles of the data sorted by intensity, was taken. The filled points in Figure 2 are these mid-averaged intensities. Since large $|\cos\theta|$ only occurs for small $|b|$, the mid-average value of $\csc|b|$ was also computed in each θ bin. The mid-averaged intensities were then fit to the form

$$I_\gamma = I_\circ + \frac{dI_\gamma}{d\csc|b|}\csc|b| + j_h(R_\circ)R_\circ\eta(l,b,0,0) \tag{14}$$

giving coefficients $I_\circ = -0.005$ photons/m^2/sec/sr, a slope of $dI_\gamma/d\csc|b| =$ 0.14 photons/m^2/sec/sr, and a local halo emissivity of $j_h(R_\circ)R_\circ = 0.037$ photons/m^2/sec/sr. This fit is the curve in Figure 2, and the contribution of the $\csc|b|$ term is shown as the open circles.

Table 1. Halo fits to the EGRET map.

$j_h(R_\circ)R_\circ$	dI_γ/dI_{100}	$dI_\gamma/d\csc\lvert b\rvert$	$r_c/R_\circ$	q^{-2}	$I_\circ$	$\sum\lvert\epsilon\rvert$
···	···	···	···	···	0.2818	413.6
0.0454	···	···	···	···	0.2006	393.5
0.1504	···	···	2.03	7.5	0	303.2
···	···	0.1075	···	···	0.1005	319.7
0.0409	···	0.1024	···	···	0.0364	298.9
0.0512	···	0.0952	0.01	1.5	0.0413	298.8
···	0.0330	···	···	···	0.1692	310.7
0.0229	0.0317	···	···	···	0.1345	303.8
0.0743	0.0183	···	2.89	5.0	0	280.9
···	0.0218	0.0574	···	···	0.1099	289.4
0.0306	0.0173	0.0656	···	···	0.0578	278.1

Note. — I_γ, $I_\circ$, $j_h R_\circ$ and ϵ are in photons/m^2/sec/sr, while I_{100} is in MJy/sr.

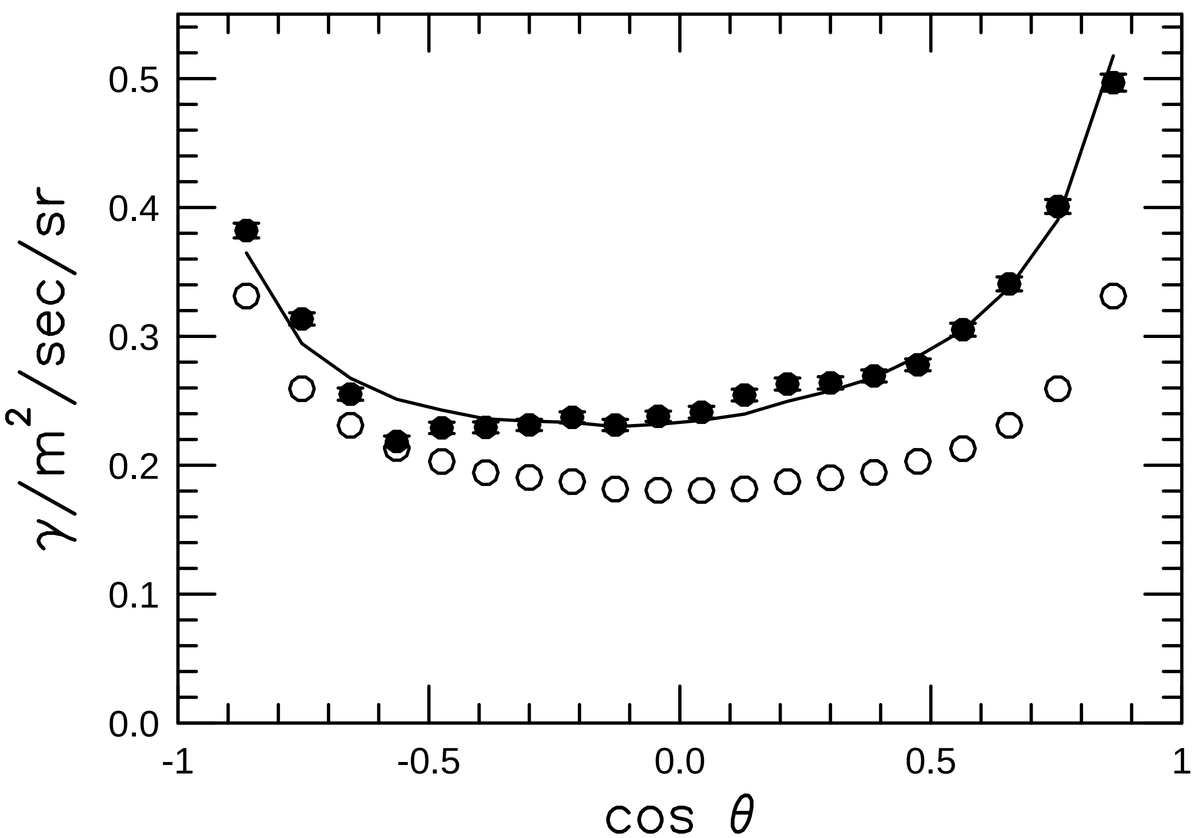

Fig. 2.— Fit of a $\csc|b|$ plus halo model to the $E > 100$ MeV intensity. θ is the angle between the line-of-sight and the galactic center.

4. Discussion

If PBH's were strongly concentrated in the halo of the Milky Way, they would produce a large anisotropic gamma ray flux which could easily be observed. A weak anisotropic signal of the predicted form is present. With the resulting value for the concentration factor $\zeta \approx (2\text{–}12)/h \times 10^5$, I can use the Halzen *et al.* (1991) calculation of the average PBH explosion rate to estimate that the explosion rate of halo PBH's is

$$\frac{dn}{dt} \leq 0.07\text{–}0.42\ \mathrm{pc}^{-3}\mathrm{yr}^{-1}. \tag{15}$$

Since there are several possible emission mechanisms other than PBH's which could be located in a galactic halo, I have taken the rate from the fits as an upper limit. The dominant uncertainty in this limit is the physical thickness of the galactic density enhancement, and this is reflected in the range of models considered in Table 1. The highest densities correspond to flattened haloes, and for a collisionless species like PBH's the highest likely flattening corresponds to an E7 galaxy shape with $q^{-2} = 11$. The best fit values obtained here when not including a separate $\csc|b|$ term,

$q^{-2} = 5$ or 7.5, are both equivalent to an E6 galaxy shape. The observed flattening of the dark matter in polar ring galaxies is in this range (Sackett *et al.* 1994).

The uncertainties in modeling the last few seconds of PBH lifetime have very little effect on the limit derived here, because the diffuse gamma ray flux comes primarily from PBH's with masses $M > 10^{14}$ gm and temperatures $kT < 100$ MeV, and radiation under these conditions is well understood. However, the behavior of PBH's at higher temperatures is not so well known, and different models of the final burst can give vastly different detection limits. For example, the recent EGRET limit of $dn/dt < 0.05$ pc^{-3}yr^{-1} (Fichtel *et al.* 1994) assumed that the last 6×10^{13} grams of PBH rest mass evaporate producing 10^{34} ergs of 100 MeV gamma rays in less than a microsecond based on the Hagedorn (1970) model for high energy particles, while in the standard model of high energy particle physics it takes $> 10^6$ years to evaporate this mass (Halzen *et al.* 1991). The particular technique used in Fichtel *et al.* (1994) would not be sensitive to standard model bursts. Porter & Weekes (1978) derived a limit of $dn/dt < 0.04$ pc^{-3}yr^{-1} using the Hagedorn model, but this limit is weakened to $dn/dt < 5 \times 10^8$ pc^{-3}yr^{-1} in the standard model (Alexandreas *et al.* 1993). Cline & Hong (1992) proposed that an expanding fireball could convert much of the 10^{34} ergs from a Hagedorn model burst into MeV gamma rays detectable by the BATSE experiment. Given the limit on dn/dt above, BATSE would have to be able to detect PBH explosions out to distances $\mathcal{O}(10^{19})$ cm if even a few percent of the BATSE bursts were due to PBH's. Other sensitive limits on the PBH explosion rate density (Phinney & Taylor 1979) depend on conversion of the last 10^{11} grams of PBH rest mass into an expanding fireball that produces a GHz radio pulse by displacing the interstellar magnetic field (Rees 1977). However, in the standard model it takes a few days for the last 10^{11} grams to evaporate (Halzen *et al.* 1991), so no radio pulse is generated.

Similarly, variations in the initial mass function of PBH's do not affect the ratio of the local emissivity to the rate density of evaporating bursts, because both the 10^{14} gm PBH's radiating the diffuse gamma rays and the 10^9 gm evaporating PBH's were initially formed with very similar masses near 10^{15} gm. Thus changing the slope of the initial mass function has very little effect on the ratio of their abundances, even though such a slope change has a large effect on the Page-Hawking limit on Ω_{PBH}.

The limit derived in the paper on the local rate-density of evaporating PBH's provides a very difficult target for all techniques to directly detect standard model PBH explosions. For example, the CYGNUS experiment presented a limit $dn/dt < 8.5 \times 10^5$ pc^{-3}yr^{-1} (Alexandreas *et al.* 1993), and my estimate is 6–7 orders of magnitude smaller.

On the other hand, the ratio of the halo density of PBH's to the Page-Hawking limit is quite close the ratio of the total halo density to the critical density in the Universe. This suggests that PBH's could be tracers of the Cold Dark Matter (CDM). This would naturally occur if the PBH's *were* the CDM, but this requires either a modified mass spectrum with an enhanced abundance of PBH's with $M > 10^{17}$ gm, or else that evaporating PBH's leave behind a stable Planck mass

remnant (MacGibbon 1987; Carr, Gilbert & Lidsey 1994). In general, the fits in this paper give concentration ratios that are slightly too high for this hypothesis if $\Omega = 1$ and $h = 0.8$. The lowest ratio of $j_h(R_\circ)R_\circ$ to $I_\circ$ in Table 1 gives a concentration of $\zeta_{low} = 8/h \times 10^4$, while if PBH's trace the dark matter the expected ratio is $(4.5 \times 10^4)/\Omega h^2$. These are equal only if $\Omega h = 0.54\zeta_{low}/\zeta$. For a more typical low value of $\zeta \approx 2/h \times 10^5$ (corresponding to $dn/dt \approx 0.1$ pc^{-3}yr^{-1}), the required value of Ωh is ≈ 0.2, which is consistent with theories of large-scale structure formation in CDM (Peacock & Dodds 1994) or CDM+Λ (Efstathiou, Sutherland & Maddox 1990) models. If this admittedly weak correspondence is correct, then 100 MeV gamma rays are providing the first non-gravitational evidence for CDM. Any model for dark matter that gives a 100 MeV gamma ray emissivity proportional to the density, such as particles with a very slow radiative decay, would also be supported by this correspondence, while models with emissivity proportional to ρ^2, such as annihilating particles, would not. More data and better galactic modeling are needed to test this exciting possibility.

One possible test is to look for gamma rays from large concentrations of dark matter. The flux from the Galaxy, $F = \int I \cos\theta d\Omega$, in Figure 1 is $F = 1.1$ γ/m^2/sec while the flux from the halo term of the best fitting model in Table 1 is $F = 0.38$ γ/m^2/sec. Scaling the latter flux to the mass and distance of M87 (Stewart *et al.* 1984), assuming a constant gamma ray luminosity to mass ratio, predicts a flux of 4×10^{-5} γ/m^2/sec for $E > 100$ MeV which is only 10 times lower than the limit of 40×10^{-5} γ/m^2/sec reported by Sreekumar *et al.* (1994). Detection of a gamma ray flux from clusters of galaxies that correlates with dark matter column density instead of gas column density would support of association of dark matter and PBH's.

This research has made use of data obtained through the Compton Observatory Science Support Center GOF account, provided by the NASA-Goddard Space Flight Center.

REFERENCES

Alexandreas, D. E. *et al.* 1993, Phys. Rev. Lett., 71, 2524.

Bertsch, D. *et al.* 1995, BAAS, 27, 820.

Carr, B. J., Gilbert, J. H & Lidsey, J. E. 1994, Phys. Rev. D, 50, 4853.

Cline, D. & Hong, W. 1992, ApJ, 401, L57.

Digel, S. W., Hunter, S. D. & Mukherjee, R. 1995, ApJ, 441, 270.

Efstathiou, G., Sutherland, W. J. & Maddox, S. J. 1990, Nature, 348, 705.

Fichtel, C. E. *et al.* 1994, ApJ, 434, 557.

Hagedorn, R. 1970, A&A, 5, 184.

Halzen, F., Zas, E., MacGibbon, J. H. & Weekes, T. C. 1991, Nature, 353, 807.

Hawking, S. W. 1974, Nature, 248, 30.

MacGibbon, J. 1987, Nature, 329, 308.

Page, D. N. & Hawking, S. W. 1976, ApJ, 206, 1.

Peacock, J. A. & Dodds, S. J. 1994, MNRAS, 267, 1020.

Phinney, S. & Taylor, J. H. 1979, Nature, 277, 117.

Porter, N. A. & Weekes, T. C. 1978, MNRAS, 183, 205.

Rees, M. J. 1977, Nature, 266, 333.

Sackett, P., Rix, H.-W., Jarvis, B. J. & Freeman, K. C. 1994, ApJ, 436, 629.

Sreekumar, P., Bertsch, D. L., Dingus, B. L., Esposito, J. A., Fichtel, C. E., Hartman, R. C., Hunter, S. D., Kanbach, G., Kniffen, D. A. & Lin, Y. C. 1994, ApJ, 426, 105.

Stewart, G., Canizares, C., Fabian, A. & Nulsen, P. 1984, ApJ, 278, 536.

Wright, E. L., Smoot, G. F., Kogut, A., Hinshaw, G., Tenorio, L., Lineweaver, C., Bennett, C. L. & Lubin, P. M. 1994, ApJ, 420, 1.

This preprint was prepared with the AAS LaTeX macros v4.0.